

RESEARCH ARTICLE | APRIL 25 2023

Ultraviolet control of bacterial biofilms in microfluidic chips

Gabriel Ramos; Clara Toulouse; Maya Rima; ... et. al



Biomicrofluidics 17, 024107 (2023)

<https://doi.org/10.1063/5.0135722>



View
Online



Export
Citation

CrossMark

Articles You May Be Interested In

Elongational rheology of bacterial biofilms in situ

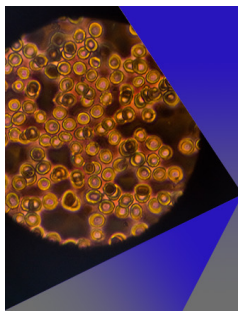
Journal of Rheology (November 2016)

A morphological study of the changes in the ultrastructure of a bacterial biofilm disrupted by an ac corona discharge in air

Journal of Applied Physics (August 2016)

Morphomechanics of bacterial biofilms undergoing anisotropic differential growth

Appl. Phys. Lett. (October 2016)



AIP Advances

Special Topic: Medical Applications
of Nanoscience and Nanotechnology

Submit Today!

AIP
Publishing

AIP
Publishing

Ultraviolet control of bacterial biofilms in microfluidic chips

Cite as: Biomicrofluidics 17, 024107 (2023); doi: 10.1063/5.0135722

Submitted: 22 November 2022 · Accepted: 4 April 2023 ·

Published Online: 25 April 2023



Gabriel Ramos,¹ Clara Toulouze,¹ Maya Rima,² Olivier Liot,¹ Paul Duru,¹ and Yohan Davit^{1,a)}

AFFILIATIONS

¹Institut de Mécanique des Fluides (IMFT), CNRS and Université de Toulouse, 31400 Toulouse, France

²Laboratoire de Génie Chimique (LGC), Université de Toulouse, CNRS, INPT, UPS, 31062 Toulouse, France

^{a)}Author to whom correspondence should be addressed: yohan.davit@imft.fr

ABSTRACT

Polydimethylsiloxane (PDMS) microfluidic systems have been instrumental in better understanding couplings between physical mechanisms and bacterial biofilm processes, such as hydrodynamic effects. However, precise control of the growth conditions, for example, the initial distribution of cells on the substrate or the boundary conditions in a flow system, has remained challenging. Furthermore, undesired bacterial colonization in crucial parts of the systems, in particular, in mixing zones or tubing, is an important factor that strongly limits the duration of the experiments and, therefore, impedes our ability to study the biophysics of biofilm evolving over long periods of time, as found in the environment, in engineering, or in medicine. Here, we develop a new approach that uses ultraviolet-C (UV-C) light-emitting diodes (LEDs) to confine bacterial development to specific zones of interest in the flow channels. The LEDs are integrated into a 3D printed light guide that is positioned upon the chip and used to irradiate germicidal UV-C directly through the PDMS. We first demonstrate that this system is successful in controlling undesired growth of *Pseudomonas aeruginosa* biofilm in inlet and outlet mixing zones during 48 h. We further illustrate how this can be used to define the initial distribution of bacteria to perturb already formed biofilms during an experiment and to control colonization for seven days—and possibly longer periods of time—therefore opening the way toward long-term biofilm experiments in microfluidic devices. Our approach is easily generalizable to existing devices at low cost and may, thus, become a standard in biofilm experiments in PDMS microfluidics.

Published under an exclusive license by AIP Publishing. <https://doi.org/10.1063/5.0135722>

I. INTRODUCTION

Bacteria primarily live within biofilms—communities of microorganisms adherent to an interface and embedded in a self-produced matrix of extracellular polymeric substances.^{1–5} Biofilms are ubiquitous on Earth^{6,7} and have a considerable impact on human health, natural environments, and industrial processes.^{2,8} They play an important role in various pathologies, including cystic fibrosis and chronic wounds.^{9,10} They drive fundamental biogeochemical processes, such as carbon¹¹ or nitrogen¹² cycles. They are also key in water processing and engineering applications, for example, in biofiltration¹³ or bioremediation.¹⁴

The behavior of a biofilm is complex and differs significantly from that of individual microorganisms that constitute it. Biofilm exhibit “emergent properties,”¹ such as enhanced resistance to antibiotics, biocides, and predators compared to free-floating planktonic bacteria. The large density of different microorganisms present in biofilms is also favorable to social interactions,⁴ which

can lead to the emergence of complex spatiogenetic patterning.¹⁵ Furthermore, biofilms are heterogeneous systems undergoing a variety of gradients,¹⁶ such as pH,¹⁷ nutrients,¹⁸ and oxygen.¹⁹ Understanding the complexity of biofilms and the many cues that drive their behavior is an open challenge overlapping biophysics, microbiology, and ecology.

Microfluidic approaches have proven to be a powerful tool in studying bacteria and biofilms (see discussion in Ref. 20). Polydimethylsiloxane (PDMS) micropatterning and microfluidics,²¹ in particular, provide the ability to precisely control the condition of development and to isolate the role of a specific phenomenon. PDMS has many advantages in microfluidic applications.²² It has excellent optical properties, is cheap, stable, non-toxic, and permeable to oxygen.^{23,24} This has made PDMS micropatterning the most widely used microfluidic tool for studying biological systems.²¹ Such technologies have brought new insight into a broad range of phenomena²⁵ including interactions of bacteria with

Downloaded from http://pubs.aip.org/journal/bmf/article-pdf/doi/10.1063/5.0135722/16998108/024107_1_5.0135722.pdf

flow,^{2,5} the effect of gradients, motility, and taxis,²⁶ communications,²⁷ and the dynamics of social interactions.²⁸

We argue that one of the limitations of current PDMS systems is their inability to confine the biofilm to a zone of interest. Over time, motile bacteria will colonize all parts of the system and form biofilm in the nutrient supplies, the tubing, the pumps, and the sensors. This has important consequences on the experiments. It may affect the quality and interpretation of the results, making it particularly difficult to control boundary conditions—e.g., how much nutrient is at the inlet if there is biofilm in the tubing? It also limits biofilm experiments to short timescales, with most experiments in microfluidic systems focusing on the early stages of biofilm development, often over a few hours,^{5,27,29} very rarely over two or three days.^{30,31} In contrast, biofilms in medical, environmental, or industrial conditions evolve over days, weeks, months, or even years. This makes it necessary to develop technologies to study them in laboratory-controlled conditions over long time scales.

Here, we develop a novel low-cost approach that allows us to confine biofilm growth to specific zones in the flow channels. We present a device consisting of ultraviolet-C (UV-C) light-emitting diodes (LEDs) integrated into a 3D printed light guide that is used to irradiate germicidal UV-C through the PDMS and confine bacterial development to specific zones of interest. Our experimental setup is detailed in Sec. II along with the material and methods used throughout the paper. To test the effectiveness of our approach, we present in Sec. III an application to a model system where *Pseudomonas aeruginosa* biofilms are grown in a network of flow channels. We also show that the same UV-C irradiation approach through the PDMS can be used to define initial conditions and generate perturbations of biofilm processes.

II. EXPERIMENTAL SETUP

A. PDMS chip

We used photolithography methods for the mold fabrication using dry film negative photoresist (EMS-Nagase DF10100) on a silicon wafer. The device was made using polydimethylsiloxane (PDMS, Sylgard 184) with a reticulant agent in a ratio 1:10 and the chip was bonded to a glass slide by means of a corona plasma wand (Electro-Technic BD-20AC Corona surface treater). The microfluidic chip consists of two mixing zones and a honeycomb channel network [Fig. 1(b)], with each channel having a cross section of $100 \times 100 \mu\text{m}^2$. Before bacterial inoculation, the microfluidic device is degassed inside the desiccator for 1 h, the channels are cleaned using ethanol, and, finally, the device is filled with fresh culture medium.

B. Culture of bacteria and inoculation of the chip

We use *Pseudomonas aeruginosa* strain ATCC 15692 GFP. The strain is collected from a -80°C stock and cultured overnight in 10 ml of Brain Heart Infusion (BHI, Merck, 37.5 g/l) with ampicillin ($300 \mu\text{g}/\text{ml}$) at 30°C and 180 RPM. The next day, part of the culture is diluted to obtain an optical density at 600 nm (OD_{600}) of 0.7. This concentration ensures bacterial attachment during the inoculation phase. Inoculation is performed by flowing simultaneously the culture medium and $\sim 100 \mu\text{l}$ of bacterial suspension using two inlets, each one at $8 \mu\text{l}/\text{min}$. After inoculation, the bacterial inlet is sealed with

silicone to avoid colonization by remaining bacteria, while the culture medium inlet continues flowing without detaching the initially adhered bacteria (see the [supplementary material](#)). Then, the flow rate is set to $2 \mu\text{l}/\text{min}$ for the rest of the experiment.

C. Flow system

Flow rate is imposed using a pressure pump (Fluigent MFCS-EZ) coupled to a flow meter (Fluigent Flow Unit S). Both the pump and the flow meter are connected to a computer and controlled by a software (Fluigent A-i-O) that continuously adapts the pressure values in order to impose a constant flow rate [Fig. 1(a)]. The culture medium flowing during the whole experiment is BHI with ampicillin ($300 \mu\text{g}/\text{ml}$) containing red passive tracers (Invitrogen FluoSpheres carboxylate $1.0 \mu\text{m}$ red 580/605) suspended in a concentration of $6.7 \mu\text{g}/\text{ml}$. Spheres can attach to the biofilm without significantly modifying colonization of the network (see the [supplementary material](#)). The temperature of the device and the culture medium is maintained at 30°C using a cage incubator (Okolab).

D. Imaging

The microfluidic device is imaged using an inverted microscope (Nikon Eclipse Ti2-E) with a 4x objective (Plan Fluor 0.13 NA) and imaged using a sCMOS camera (PCOedge 4.2bi). Time-lapse microscopy is performed by taking images automatically every hour using the JOBS® module from NIS-Elements AR. Images are taken in bright field (BF, 30 ms exposure time) and in green fluorescence (GFP, 80 ms exposure time). For fluorescence images, a light source (Lumencor Sola light engine SM at 10%) filtered by a cube (Nikon filter cube GFP-3035D) excites the green fluorescence protein produced by the bacteria (GFPmut3).

In order to observe the fluid flow paths complementary to direct biofilm imaging, Particle Tracking Velocimetry (PTV) is performed using the red passive fluorescent tracers suspended in the culture medium and recorded using a fast camera (PCO Dimax) during 170 ms at 100 fps and 2 ms exposure time. The Sola light source for fluorescence was at 100% to improve the image contrast due to the high speed of the particles, and a cube (MXR00708 TRITC-B 32 mm) filtered the light to excite the tracers.

Both biofilm images and PTV videos are performed in mosaic, scanning 30 positions to reconstruct the final image. The total scanning time is of the order of seconds, while the typical doubling time of bacteria in rich medium is between 25 and 35 min,³² and, hence, there are no changes of the global state of the chip between the first and the last image of the mosaic.

E. UV-C irradiation device for inlet and outlet

Two UV-C LED sources (CHTPON 1 W-20 mm-120°) irradiating at 275 nm are attached to a 3D printed piece containing a special UV mirror (Edmund Optics TECHSPEC® $20 \times 20 \text{ mm}^2$) in order to constantly expose the mixing zones of the device to UV-C light [Fig. 1(c) and purple areas in Fig. 1(d)]. Intensity of UV-C LEDs is regulated by a homemade electronic controller connected to a computer. *In situ* measurements of the irradiance were performed on every mixing zone using a photo/radiometer (Delta Ohm Portable Luxmeter HD 2102.1) connected to a UV-C probe

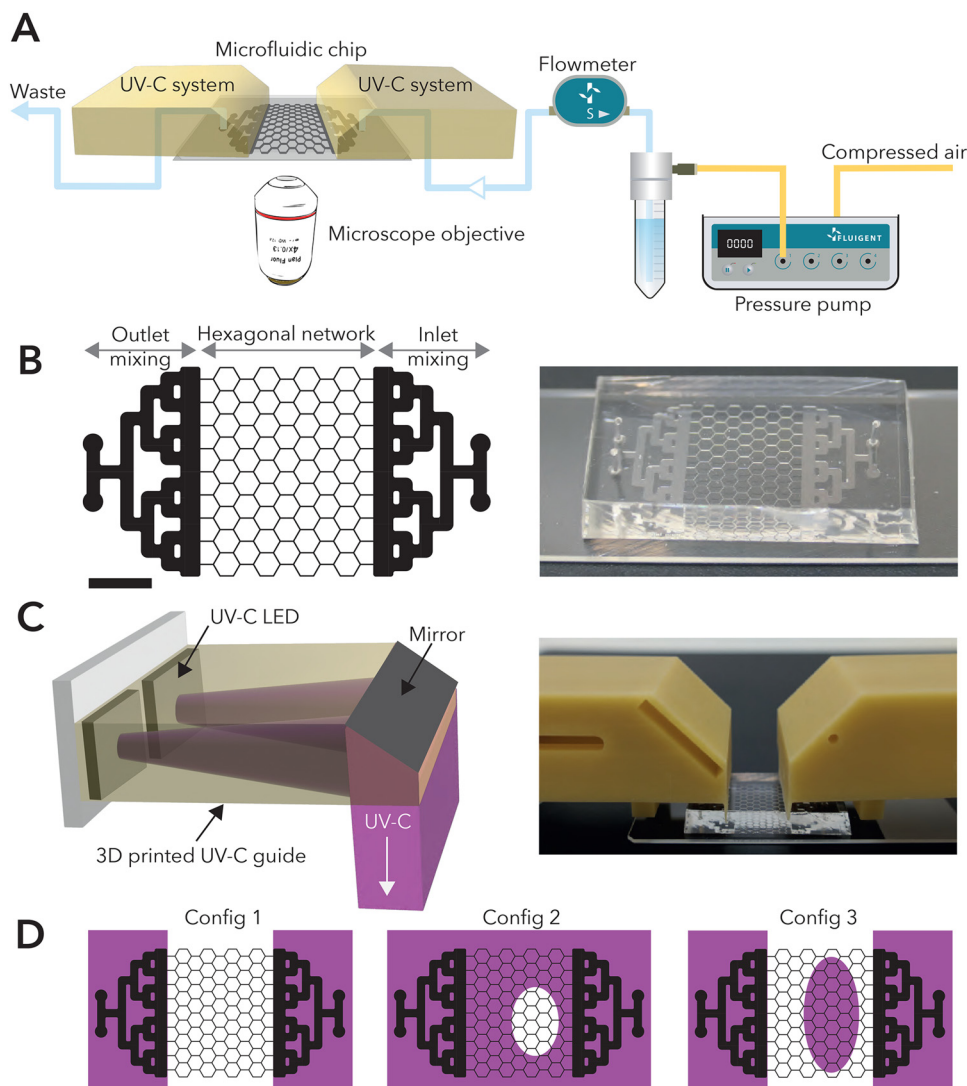


FIG. 1. Experimental setup. (a) Schematics of the fluidic system. A constant flow rate is imposed through the microfluidic chip using a pressure pump coupled with a flow meter. Image acquisition is performed every hour with an inverted microscope using a 4× objective. Two UV-C systems irradiate both the inlet and outlet of the chip during the total duration of the experiment. (b) Microfluidic chip. On the left, the schematic shows the different regions: the mixing zones (inlet and outlet) and the hexagonal network channels. On the right, we present a picture of the micro-patterned PDMS plasma bonded directly to a glass slide. Scale bar is 5 mm. (c) UV-C device. The schematic on the left shows a pair of UV-C LEDs attached to a 3D printed guide with a mirror on its edge that reflects the UV-C light onto the desired zones. On the right, an actual image of the positioning of the UV-C system is presented. (d) Irradiated zones on the chip (purple zones) for three different UV-C configurations used in the experiments. No network irradiation (Config 1), control of initial conditions (Config 2), and perturbation on the network (Config 3). In Config 2, a small aluminum cylinder blocks the light to protect part of the network exposed to a central UV-C LED, while in Config 3, an aluminum plate with a hole in its center allows the irradiation of a portion of the network. The resulting patterns are not circular in the protected zone in Config 2 and in the irradiated zone in Config 3 because the angle of incidence of the central UV-C light was slightly deviated from the normal to the PDMS surface.

(Delta Ohm LP471UVC irradiance probe). The transmittance we measured through a 4 mm PDMS layer is about 54%, yielding an irradiance of $\sim 9.3 \mu\text{W}/\text{cm}^2$ on the mixing zone. Considering that an element of fluid takes ~ 172.5 s to go through the mixing zone at the flow rate studied in this article ($2 \mu\text{l}/\text{min}$), we estimate that the dose received by the culture media before being consumed by bacteria is $\sim 1.6 \text{ mJ}/\text{cm}^2$. We performed experiments at different doses to test the impact of UV-C on culture media (0, 12.9, and $129 \text{ mJ}/\text{cm}^2$), and we did not observe any significant influence on the viability of cell culture. For more details, see the [supplementary material](#).

F. UV-C irradiation for initial condition and perturbations

A third UV-C source irradiating at 265 nm is directly placed above the microfluidic device (Klaran, 70 mW KL265-50V-SM-WD) to control initial conditions and perform perturbations on the system

[Configs 2 and 3 in Fig. 1(d)]. In both cases, the LED is irradiating at $138 \mu\text{W}/\text{cm}^2$. To control initial conditions, the central UV-C LED is on for 20 h from the beginning of the experiment and then is removed. In order to protect a portion of the network from UV-C radiation, an aluminum-made obstacle is placed onto the microfluidic device [Config 2 in Fig. 1(d)]. To perform perturbations, the central UV-C LED is turned on after 14 h of biofilm development. The irradiation is performed for 24 h and then the UV-C LED was removed to let the biofilm develop again. To define the region to be perturbed, an aluminum-made plate with a hole in its center is placed onto the microfluidic device [Config 3 in Fig. 1(d)].

G. Image processing

Fluorescence images were treated using Fiji³³ to subtract the background and adjust the contrast for biofilm visualization. Bright field images were processed with homemade Matlab scripts for

Downloaded from http://pubs.aip.org/aip/bmf/article-pdf/doi/10.1063/5.0135722/16998108/024107_1_5.0135722.pdf

increasing the image intensity of the mixing zones, which received less illumination due to the presence of the UV-C system, and for improving the contrast between the background and the channels by the application of a mask on the image. PTV images were treated by subtracting the background and then detecting particles using a custom Python script. The reconstruction of trajectories was performed in Matlab using an optimization algorithm (Hungarian algorithm). Resulting PTV images were created with homemade scripts in Matlab, overlaying the detected particle tracks with the average image of the video. The relative intensity of GFP fluorescence was computed by adding pixel intensities over either the inlet or outlet mixing zones after noise filtering and normalization by the maximum pixel intensity found on the image sequence.

III. RESULTS AND DISCUSSION

A. UV-C irradiation prevents colonization of the mixing zones

We first aim at validating our approach by comparing biofilm growth in microfluidic chips with (Config 1) and without using our device to irradiate UV-C in the inlet and outlet mixing zones. Experiments consisted in inoculating GFP-tagged *P. aeruginosa* in the channels, then flowing the culture medium at $2 \mu\text{l}/\text{min}$ to let the biofilm grow and visualizing growth through time-lapse fluorescence and bright field microscopy. In the case with UV-C, the

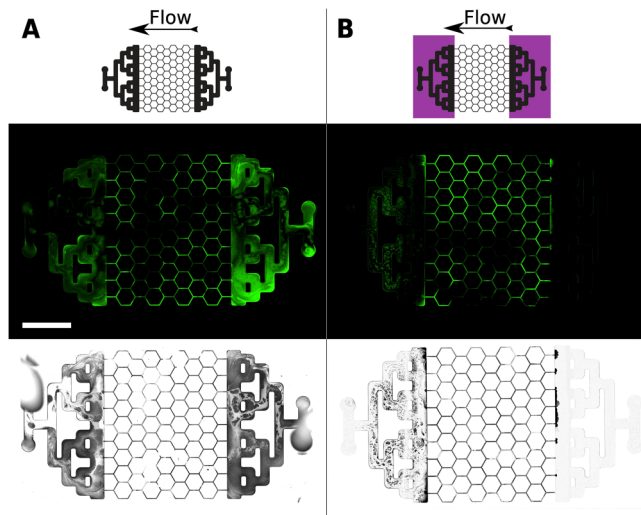


FIG. 2. UV-C can be used to prevent inlet colonization and to limit outlet biofilm attachment. The schematics show the area irradiated by the UV-C LEDs (purple color) with arrows indicating the direction of the flow. Fluorescence images are on the top (black and green) and bright field images (gray levels) on the bottom. (a) Fully developed biofilm after 48 h without UV-C. Brighter green regions in fluorescence and darker regions in bright field indicate biofilms. Without UV-C, the biofilm is fully colonizing the mixing zones at both the inlet and outlet. (b) Fully developed biofilm after 48 h using UV-C LEDs. The inlet is clean and the biofilm on the outlet, which comes from detachments within the network, is limited by the UV-C irradiation. Both experiments were performed at $2 \mu\text{l}/\text{min}$ at 30°C . The scale bar is 5 mm.

illumination of the inlet and outlet mixing zones is constant throughout the experiment. Figure 2 shows images after 48 h of growth with flow from right to left and Fig. 3 the integrated fluorescence intensity over inlet and outlet mixing zones after 42 h for triplicates. In the inlet mixing zone, we see that the chip without UV-C has a large quantity of biomass (mean intensity 0.80 a.u. in Fig. 3 after 42 h) with visible streamers (i.e., filamentous biofilm structures following the flow) and channels that seem entirely clogged. Biofilm was also visible to the naked eye in the inlet tubing, showing that motile bacteria had traveled against the flow for colonization. On the contrary, in the chip with UV-C, the inlet mixing zone is almost completely clean (mean intensity 0.11 a.u. in Fig. 3 after 42 h). UV-C irradiation inactivates free-floating and initially attached bacterial cells by interfering with transcription and replication.³⁴ Biofilm only managed to slightly grow against the flow from the first channels of the hexagonal network and appear as small mushroom-like structures. These structures seemed to “burst” upon reaching the zone with strong UV illumination (see Movie 1 in the supplementary material). No biofilm was visible in the inlet tubing.

For the outlet, we again observe that a large quantity of biomass has formed in the case without UV-C (mean intensity 0.54 a.u. in Fig. 3 after 42 h). In the case with UV-C, biofilm managed to attach to the PDMS and glass, which was not the case for the inlet. However, the quantity of biofilm is smaller than in the case without UV-C, thus showing that the irradiation is efficient in controlling the formation of biofilms but cannot prevent it completely (mean intensity 0.20 a.u. in Fig. 3 after 42 h). It has been previously shown that the biofilm matrix can act as a shield to UV-C irradiation.^{35,36} Since we observed regular detachment of

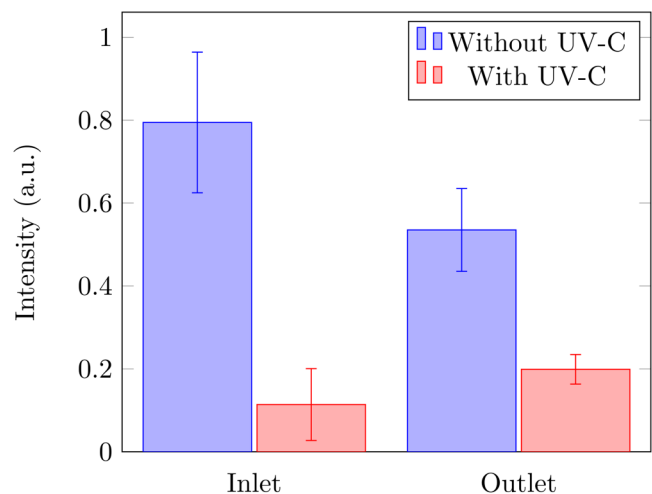


FIG. 3. Relative intensity of GFP fluorescence in arbitrary unit (a.u.) integrated over the inlet and outlet mixing zones with and without UV-C irradiation after 42 hours at $2 \mu\text{l}/\text{min}$ and 30°C . The histogram shows the average values of triplicates with standard error. Without UV-C, the values are 0.80 ± 0.17 (Inlet) and 0.54 ± 0.10 (Outlet). With UV-C, the values are 0.11 ± 0.09 (Inlet) and 0.20 ± 0.04 (Outlet).

Downloaded from http://pubs.aip.org/aip/bmf/article-pdf/doi/10.1063/5.0135722/16998108/024107_1_5.0135722.pdf

large patches of biofilm from the hexagonal network, we hypothesize that bacteria visible at the outlet are much more resilient to UV-C because they initially formed in the network and then got transported in the mixing zone. This was not observed in the inlet because bacteria are either initially present from the inoculation or move to this zone using their bulk or surface motility. Therefore, bacteria at the inlet are irradiated in their planktonic state and never have the opportunity to form a biofilm that would shield them from part of the UV-C.

B. UV-C irradiation control boundary conditions

To further assess the effect of the UV-C, we now study the impact of biofilm colonization in the mixing zones on the flow. We want to determine whether flow in the zone of interest is perturbed by biomass forming in the mixing zones and whether UV-C irradiation can modify flow boundary conditions. The idea is that the pressure distribution at the inlet and outlet of the network should be approximately uniform. The flow, on the other hand, should be controlled by the distribution of hydraulic conductivities in the network, which locally scales with the channel hydraulic radius as r_h^4 , and thus strongly depends on the amount of biofilm in each branch.

Figure 4 compares the trajectories of fluorescent microparticles with and without UV-C. In the case without UV-C, particles are localized in specific zones of the system and only a single flow channel has formed through the structure. This is a common trend observed when the inlet mixing zone is colonized (see Sec. 6 in the supplementary material). We hypothesize that the unwanted clogging is such that the conductivity of channels in the mixing zones is driving the flow, not growth in the hexagonal network. In the case with UV-C, particles have been transported almost everywhere in both mixing zones and several flow channels have formed through the zone of interest. This suggests that UV-C is efficient in controlling boundary conditions of the zone of interest.

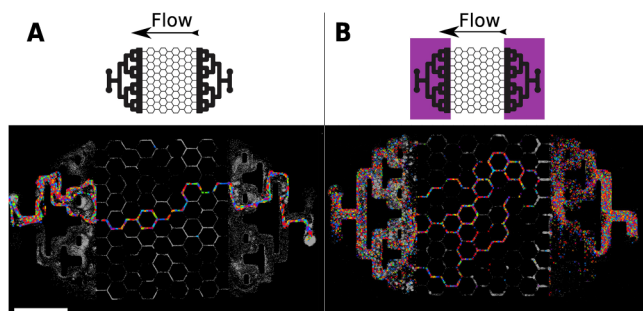


FIG. 4. UV-C can be used to control boundary conditions. Using particle tracking velocimetry (PTV), we observe the flow paths through the microfluidic system. Each color represents a detected trajectory of one tracer particle. (a) Experiment without UV-C. The biofilm developed in the mixing zones drives the flow through the network with a single channel. (b) Experiment with UV-C. Clogging in the mixing zones is negligible and flow is controlled by hydraulic conductivities in the hexagonal network. Both experiments show the biofilm formation 48 h after the inoculation at 30 °C and 2 μ l/min. Scale bar 5 mm.

Beyond flow, the presence of a large quantity of biomass in the inlet mixing zone and in the tubing is also expected to strongly modify mass transport and induce, in particular, uncontrolled nutrient uptake before the network. This would lead to difficulties in the interpretation of the results with most nutrients being consumed before reaching the hexagonal network. In that sense, we see that we will have a much more homogeneous condition in the case with UV-C.

C. UV-C irradiation can be used to control initial conditions

The optical approach to controlling the spatial distribution of the biomass can be used for other purposes and we provide example applications in Secs. III C, D, and E. As an illustration, we show here that we can initially localize bacteria to a specific portion of the zone of interest. To do so, we performed the same inoculation procedure, but then illuminated the hexagonal network with a separate UV-C LED, using a mask to shield part of the illumination. The idea was that we should have active bacteria only in the zone that was protected from UV-C, and, thus, that we can define the initial boundary of the growth problem. Fig. 5 shows the time-lapse images in green fluorescence and bright field after 1, 20, 30,

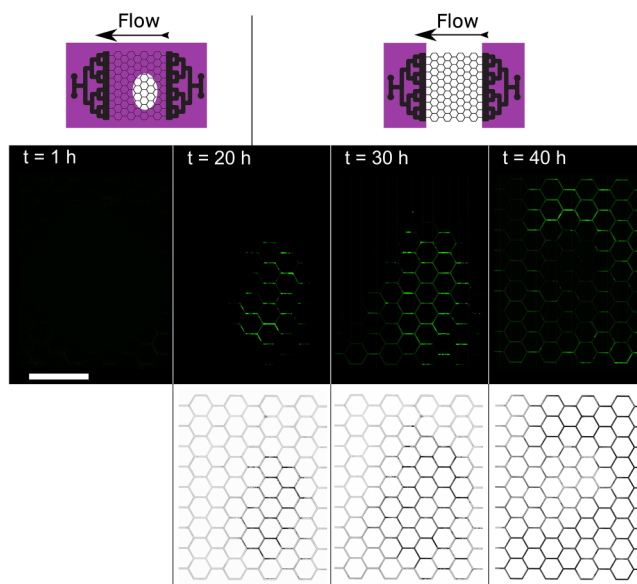


FIG. 5. UV-C can be used to control bacterial localization at initial times. The drawing shows the area irradiated by the UV-C led (purple color), the top row shows the images in fluorescence and the bottom row the images in bright field. The first bright field image is missing, because the UV-C LED above the device is blocking the white light from the microscope. The central UV-C LED was operational above the device for 20 h after inoculation and then was removed. During this first stage of the experiment, UV-C irradiation prevented biofilm formation everywhere except in the protected region (bright green zones in fluorescence and dark zones in bright field). After UV-C removal, from 20 to 40 h, the biofilm starts expanding and colonizes the rest of the device. The experiment was performed at 30 °C and 2 μ l/min. Scale bar 5 mm.

Downloaded from http://pubs.aip.org/aip/bmf/article-pdf/doi/10.1063/5.0135722/16998108/024107_1_5.0135722.pdf

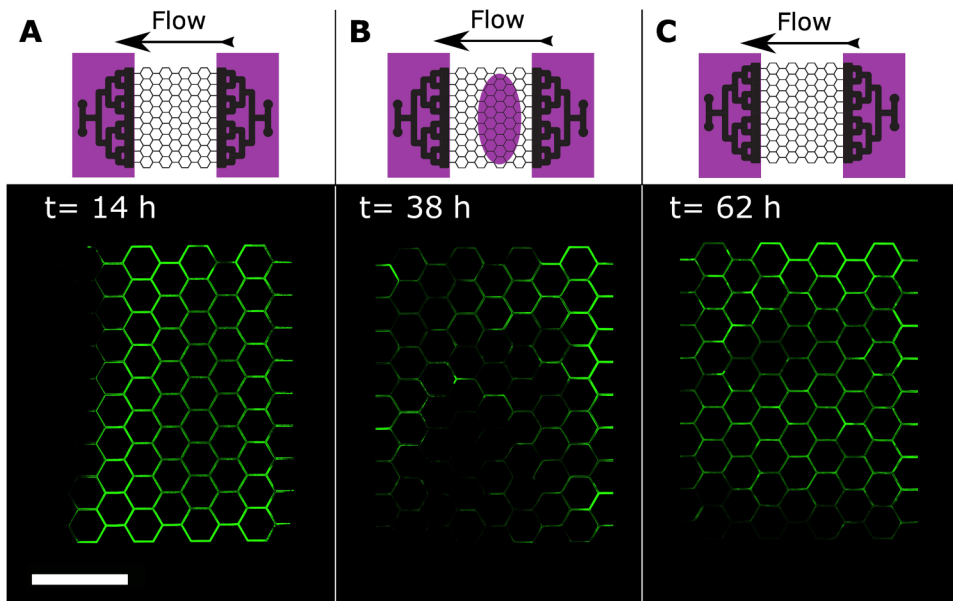


FIG. 6. UV-C can be used to generate perturbations of a fully grown biofilm. (a) Biofilm development 14 h after the inoculation, just before the start of the UV-C irradiation. (b) State of the biofilm after 24 h of UV-C irradiation (38 h after the inoculation). The drawing shows the area irradiated by the UV-C. At this moment, the UV-C led was just turned off. (c) Recolonization of the biofilm 24 h after UV-C removal. The experiment was performed at 30 °C at 2 μ l/min. Scale bar 5 mm.

and 40 h of growth. We indeed see that biofilm initially forms in the zone shielded from UV-C. The mechanism here is the same as in the inlet (see Fig. 2). Bacteria damaged by the UV-C are evacuated from the channels with the flow, while cells that were shielded are able to form biofilms. We then observe a second phase with a more complex dynamics at about 40 h, when bacteria have had time to colonize the rest of the system and biofilm has started forming everywhere in the network.

D. UV-C irradiation can be used to induce perturbations

We further wanted to determine whether UV-C could be used to perturb an already formed biofilm, which is a much more difficult problem than just changing the initial conditions. In the case of the initial conditions, only individual bacteria or small microcolonies had formed in the network and we have seen in Sec. III A

that the efficiency of the UV-C treatment depends upon the maturity of the biofilm. Here, we proceeded to growing biofilm in the zone of interest without any UV-C for 14 h and then illuminating this zone with UV-C for 24 h (Fig. 6). We observed important changes in the spatial distribution of the biofilm through the network with a significant decrease of the total biomass. Upon stopping the UV-C and letting growth continue, we also recovered biofilm everywhere in the system with a distribution reminiscent to that after 14 h.

E. UV-C irradiation makes week-long experiments possible

One of the main goals of this paper was to determine whether the UV-C illumination could be used to perform longer term biofilm experiments in microfluidic systems. To test this, we reproduced the experiment in Fig. 2 twice over both 5 days and

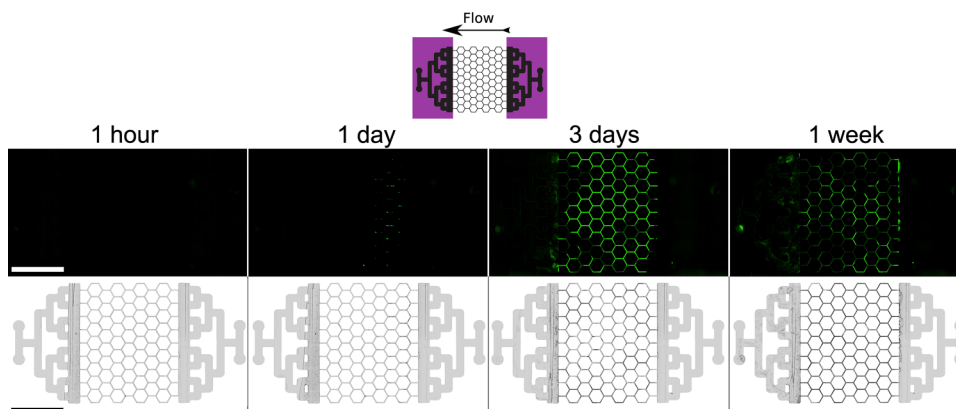


FIG. 7. UV-C irradiation allows week-long experiments. Fluorescent images are on the top and bright field images on the bottom. We see that bacteria grow within the zone of interest but the inlet remains clean even after one week of growth. The outlet shows a limited number of biofilm patches due to detachments within the network and transport by the flow, but their growth is controlled by the UV-C light (see also Movie 2 in the supplementary material). The experiment was performed at 30 °C and 2 μ l/min. Scale bar 5 mm.

Downloaded from http://pubs.aip.org/journal/bmf/article-pdf/doi/10.1063/5.0135722/16998108/024107_1_5.0135722.pdf

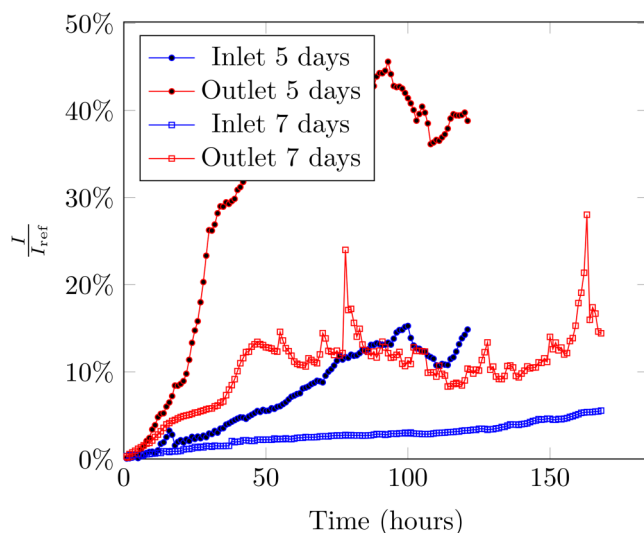


FIG. 8. Relative intensity of GFP fluorescence for the inlet and outlet mixing zones during 5 and 7 days. The intensity (I) is expressed as a percentage of the maximum fluorescence integrated over the inlet mixing zone (I_{ref}) in the case without UV-C (Figs. 2 and 3). The inlet shows a slow increase corresponding to the growth of the mushroom-like structures at the inlet of the hexagonal network. The inlet and outlet intensity in the case of 5 days increase faster due to a slight translation in the positioning of the UV-C system, which allowed more colonization at the boundary with the hexagonal network. The outlet shows biomass attached in the mixing zones and fluctuations corresponding to detachment from the hexagonal network. The experiment was performed at 30 °C and 2 $\mu\text{l}/\text{min}$ (same as in Fig. 7).

an entire week. For the week-long experiment, results in Figs. 7 and 8 show that the colonization of mixing zones after 1 week is similar to that after 3 days, with almost no biomass in the inlet mixing zone and little biofilm in the outlet. In the case of the 5 days experiment, the UV-C system was not perfectly aligned with the boundary of the hexagonal network. It thus allowed biofilm to grow from the network into the mixing zones forming a layer of biofilm on the boundary (Sec. 7 in the [supplementary material](#)), with a significant impact upon the results. Even though the time-lapse imaging still shows that colonization remains controlled in the rest of the mixing zones, this case shows that the UV-C system should be positioned carefully.

IV. CONCLUSIONS AND OUTLOOK

Ultraviolet-C, particularly in the range 250–270 nm, have long been known to damage the genetic material of microorganism and, thus, to be germicidal.³⁴ The advent of UV-C light-emitting diodes^{37,38} has made it possible to develop new approaches to mitigating microorganisms growth, for instance, in water resources management.^{39,40} In this paper, we have shown that UV-C LEDs combined with masks and simple light guides can be used to delineate bacterial growth to a specific zone of interest in microfluidic channels. Our approach takes advantage of the transparency of PDMS to UV-C to illuminate specific zones of the system directly

through the PDMS. We have used this approach to eliminate bacterial growth outside the area of interest in the flow system and to control the initial and boundary conditions of the zone of interest. Further, we have also shown that this allows us to perform microfluidic experiments without colonization of the tubing or mixing zones for 7 days. When the UV-C system was positioned properly, the state of the colonization after 3 or 7 days was similar, thus suggesting that experiments could be run for an even longer period of time, possibly several weeks. This may open the way toward long-term biofilm experiments in microfluidic devices.

One limitation is the ability to prevent growth and attachment of already formed biofilms. Extracellular polymeric substances partly protect bacteria from UV-C so that some biofilm pre-formed in the hexagonal network was able to subsist in the outlet. However, our system was able to efficiently prevent further growth and thus control the impact on the flow. For *P. aeruginosa*, a dose of 4 mJ/cm^2 is enough for a 2 log inactivation.⁴⁰ Since our irradiance in the mixing zones was about 9.3 $\mu\text{W}/\text{cm}^2$, a 2 log inactivation is thus expected in about 7 min. However, the same dose is less efficient for an already formed biofilm, reaching about 1 log inactivation.³⁷ Even with increased irradiance (138 $\mu\text{W}/\text{cm}^2$ in our case and 102 $\mu\text{W}/\text{cm}^2$ in Ref. 37), there is no complete inactivation of the already formed biofilm, because of the protection offered by the extracellular polymeric substances. On the other hand, *P. aeruginosa* is known to produce a large amount of extracellular polymeric substances and is more resistant to UV-C irradiation than other bacteria, including *E. coli*⁴⁰ for example. Since our approach does not require any integration directly to the chip, it can be used for a broad range of organisms and systems without costly changes to existing designs. If a higher level of control is required, one could increase the power of the UV-C illumination, for instance, by increasing the number of LEDs—of course, heat dissipation would have to be dealt with properly. The guiding optics for UV-C could also be improved to gain in efficiency and to provide a finer control of the exact positioning of the irradiated zone, the UV-C power delivered to the sample and the uniformity of intensity distribution. This would broaden the range of potential applications of this technology.

SUPPLEMENTARY MATERIAL

See the [supplementary material](#) for more details about experimental methods and effects of UV-C on growing biofilm.

ACKNOWLEDGMENTS

This work is part of a project that has received funding from the European Research Council (ERC) under the European Union's Horizon 2020 research and innovation programme (Grant Agreement No. 803074). The authors thank Julien Lefort and Emmanuel Libert for their contribution to the design and fabrication of the UV-C system and Christophe Coudret for fruitful discussions. Photolithography for the mold fabrication has been done at LAAS-CNRS (No. UPR8001).

AUTHOR DECLARATIONS

Conflict of Interest

The authors have no conflicts to disclose.

Author Contributions

Gabriel Ramos: Conceptualization (equal); Data curation (lead); Formal analysis (lead); Investigation (lead); Methodology (lead); Software (equal); Visualization (lead); Writing – original draft (equal). **Clara Toulouze:** Conceptualization (supporting); Data curation (supporting); Investigation (supporting); Methodology (supporting). **Maya Rima:** Data curation (supporting); Investigation (supporting); Methodology (supporting). **Olivier Liot:** Conceptualization (equal); Methodology (supporting); Software (equal); Supervision (supporting); Writing – original draft (supporting). **Paul Duru:** Conceptualization (equal); Methodology (supporting); Supervision (supporting); Writing – original draft (supporting). **Yohan Davit:** Conceptualization (equal); Data curation (equal); Formal analysis (equal); Funding acquisition (lead); Project administration (lead); Supervision (lead); Writing – original draft (equal).

DATA AVAILABILITY

The data that support the findings of this study are available from the corresponding author upon reasonable request.

REFERENCES

- ¹H.-C. Flemming, J. Wingender, U. Szewzyk, P. Steinberg, S. A. Rice, and S. Kjelleberg, “Biofilms: An emergent form of bacterial life,” *Nat. Rev. Microbiol.* **14**(9), 563–575 (2016).
- ²A. L. M. Chun, A. Mosayyebi, A. Butt, D. Carugo, and M. Salta, “Early biofilm and streamer formation is mediated by wall shear stress and surface wettability: A multifactorial microfluidic study,” *MicrobiologyOpen* **11**(4), e1310 (2022).
- ³V. Gordon, M. Davis-Fields, K. Kovach, and C. Rodesney, “Biofilms and mechanics: A review of experimental techniques and findings,” *J. Phys. D: Appl. Phys.* **50**, 223002 (2017).
- ⁴C. D. Nadell, J. B. Xavier, and K. R. Foster, “The sociobiology of biofilms,” *FEMS Microbiol. Rev.* **33**(1), 206–224 (2009).
- ⁵G. Savorana, J. Słomka, R. Stocker, R. Rusconi, and E. Secchi, “A microfluidic platform for characterizing the structure and rheology of biofilm streamers,” *Soft Matter* **18**(20), 3878–3890 (2022).
- ⁶H.-C. Flemming and S. Wuerzt, “Bacteria and archaea on Earth and their abundance in biofilms,” *Nat. Rev. Microbiol.* **17**(4), 247–260 (2019).
- ⁷Y. Bar-On, R. Phillips, and R. Milo, “The biomass distribution on Earth,” *PNAS* **115**, 6506–6511 (2017).
- ⁸M. Pousti, M. P. Zarabadi, M. A. Amirdehi, F. Paquet-Mercier, and J. Greener, “Microfluidic bioanalytical flow cells for biofilm studies: A review,” *Analyst* **144**(1), 68–86 (2018).
- ⁹L. Hall-Stoodley, P. Stoodley, S. Kathju, N. Høiby, C. Moser, J. William Costerton, and A. Moter, “Towards diagnostic guidelines for biofilm-associated infections,” *FEMS Immunol. Med. Microbiol.* **65**, 127–145 (2012).
- ¹⁰S. Subramanian, R. C. Huiszoon, S. Chu, W. E. Bentley, and R. Ghodssi, “Microsystems for biofilm characterization and sensing – A review,” *Biofilm* **2**, 100015 (2020).
- ¹¹N. B. Justice, C. Pan, R. Mueller, S. E. Spaulding, V. Shah, C. L. Sun, A. P. Yelton, C. S. Miller, B. C. Thomas, M. Shah, N. VerBerkmoes, R. Hettich, and J. F. Banfield, “Heterotrophic archaea contribute to carbon cycling in low-pH, suboxic biofilm communities,” *Appl. Environ. Microbiol.* **78**(23), 8321–8330 (2012).
- ¹²D. Wang, A. Xu, C. Elmerich, and L. Z. Ma, “Biofilm formation enables free-living nitrogen-fixing rhizobacteria to fix nitrogen under aerobic conditions,” *ISME J.* **11**(7), 1602–1613 (2017).
- ¹³A. Maurya, M. Kumar Singh, and S. Kumar, “Biofiltration technique for removal of waterborne pathogens,” in *Waterborne Pathogens* (Butterworth-Heinemann, 2020), pp. 123–141.
- ¹⁴S. Mishra, Y. Huang, J. Li, X. Wu, Z. Zhou, Q. Lei, P. Bhatt, and S. Chen, “Biofilm-mediated bioremediation is a powerful tool for the removal of environmental pollutants,” *Chemosphere* **294**, 133609 (2022).
- ¹⁵C. Nadell, K. Drescher, and K. Foster, “Spatial structure, cooperation and competition in biofilms,” *Nat. Rev. Microbiol.* **14**, 589–600 (2016).
- ¹⁶J. Wimpenny, W. Manz, and U. Szewzyk, “Heterogeneity in biofilms,” *FEMS Microbiol. Rev.* **24**(5), 661–671 (2000).
- ¹⁷J. M. Vroom, K. J. De Grauw, H. C. Gerritsen, D. J. Bradshaw, P. D. Marsh, G. Keith Watson, J. J. Birmingham, and C. Allison, “Depth penetration and detection of pH gradients in biofilms by two-photon excitation microscopy,” *Appl. Environ. Microbiol.* **65**(8), 3502–3511 (1999).
- ¹⁸A. Dal Co, S. van Vliet, and M. Ackermann, “Emergent microscale gradients give rise to metabolic cross-feeding and antibiotic tolerance in clonal bacterial populations,” *Philos. Trans. R. Soc. B* **374**, 20190080 (2019).
- ¹⁹A. D. Klementiev, Z. Jin, and M. Whiteley, “Micron scale spatial measurement of the O₂ gradient surrounding a bacterial biofilm in real time,” *mBio* **11**, e02536-20 (2020).
- ²⁰Y. Yawata, J. Nguyen, R. Stocker, and R. Rusconi, “Microfluidic studies of biofilm formation in dynamic environments,” *J. Bacteriol.* **198**(19), 2589–2595 (2016).
- ²¹D. B. Weibel, W. R. Diluzio, and G. M. Whitesides, “Microfabrication meets microbiology,” *Nat. Rev. Microbiol.* **5**, 209–218 (2007).
- ²²M. Kiran Raj and S. Chakraborty, “PDMS microfluidics: A mini review,” *J. Appl. Polym. Sci.* **137**, 48958 (2020).
- ²³A. P. Vollmer, R. F. Probst, R. Gilbert, and T. Thorsen, “Development of an integrated microfluidic platform for dynamic oxygen sensing and delivery in a flowing medium,” *Lab Chip* **5**(10), 1059 (2005).
- ²⁴T. Miranda, A. Souza, P. Sousa, J. Ribeiro, E. M. S. Castanheira, R. Lima, and G. Minas, “Properties and applications of PDMS for biomedical engineering: A review,” *J. Funct. Biomater.* **13**(1), 2 (2021).
- ²⁵R. Rusconi, M. Garren, and R. Stocker, “Microfluidics expanding the frontiers of microbial ecology,” *Annu. Rev. Biophys.* **43**, 65–91 (2014).
- ²⁶T. Ahmed, T. S. Shimizu, and R. Stocker, “Microfluidics for bacterial chemotaxis,” *Integr. Biol.* **2**(11–12), 604–629 (2010).
- ²⁷M. K. Kim, F. Ingremeau, A. Zhao, B. L. Bassler, and H. A. Stone, “Local and global consequences of flow on bacterial quorum sensing,” *Nat. Microbiol.* **1**, 15005 (2016).
- ²⁸F. J. H. Hol and C. Dekker, “Zooming in to see the bigger picture: Microfluidic and nanofabrication tools to study bacteria,” *Science* **346**(6208), 1251821 (2014).
- ²⁹J. A. Aufrecht, J. D. Fowlkes, A. N. Bible, J. Morrell-Falvey, M. J. Doktycz, and S. T. Retterer, “Pore-scale hydrodynamics influence the spatial evolution of bacterial biofilms in a microfluidic porous network,” *PLoS One* **14**(6), 1–17 (2019).
- ³⁰K. Z. Coyte, H. Tabuteau, E. A. Gaffney, K. R. Foster, and W. M. Durham, “Microbial competition in porous environments can select against rapid biofilm growth,” *Proc. Natl. Acad. Sci. U.S.A.* **114**, E161–E170 (2017).
- ³¹Y. Yawata, O. X. Cordero, F. Menolascina, J.-H. Hehemann, M. F. Polz, and R. Stocker, “Competition–dispersal tradeoff ecologically differentiates recently speciated marine bacterioplankton populations,” *Proc. Natl. Acad. Sci. U.S.A.* **111**(15), 5622–5627 (2014).
- ³²L. Yang, J. A. J. Haagensen, L. Jelsbak, H. Krogh Johansen, C. Sternberg, N. Høiby, and S. Molin, “In situ growth rates and biofilm development of *Pseudomonas aeruginosa* populations in chronic lung infections,” *J. Bacteriol.* **190**(8), 2767–2776 (2008).

- ³³J. Schindelin, I. Arganda-Carreras, E. Frise, V. Kaynig, M. Longair, T. Pietzsch, S. Preibisch, C. Rueden, S. Saalfeld, B. Schmid, J.-Y. Tinevez, D. J. White, V. Hartenstein, K. Eliceiri, P. Tomancak, and A. Cardona, "Fiji: An open-source platform for biological-image analysis," *Nat. Methods* **9**(7), 676–682 (2012).
- ³⁴R. V. Pereira, M. L. Bicalho, V. S. Machado, S. Lima, A. G. Teixeira, L. D. Warnick, and R. C. Bicalho, "Evaluation of the effects of ultraviolet light on bacterial contaminants inoculated into whole milk and colostrum, and on colostrum immunoglobulin g," *J. Dairy Sci.* **97**(5), 2866–2875 (2014).
- ³⁵C. C. R. de Carvalho, "Biofilms: Microbial strategies for surviving UV exposure," in *Advances in Experimental Medicine and Biology* (Springer International Publishing, 2017), pp. 233–239.
- ³⁶M. O. Elasri and R. V. Miller, "Study of the response of a biofilm bacterial community to UV radiation," *Appl. Environ. Microbiol.* **65**(5), 2025–2031 (1999).
- ³⁷H. Torkzadeh and E. L. Cates, "Biofilm growth under continuous UVC irradiation: Quantitative effects of growth conditions and growth time on intensity response parameters," *Water Res.* **206**, 117747 (2021).
- ³⁸S. L. Gora, K. D. Rauch, C. Carolina Ontiveros, A. K. Stoddart, and G. A. Gagnon, "Inactivation of biofilm-bound *Pseudomonas aeruginosa* bacteria using UVC light emitting diodes (UVC LEDs)," *Water Res.* **151**, 193–202 (2019).
- ³⁹B. Ma, S. Seyedi, E. Wells, D. McCarthy, N. Crosbie, and K. G. Linden, "Inactivation of biofilm-bound bacterial cells using irradiation across UVC wavelengths," *Water Res.* **217**, 118379 (2022).
- ⁴⁰S. Rattanakul and K. Oguma, "Inactivation kinetics and efficiencies of UV-LEDs against *pseudomonas aeruginosa*, *legionella pneumophila*, and surrogate microorganisms," *Water Res.* **130**, 31–37 (2018).